HAL
archives-ouvertes.fr

The nature of quasistatic deformation in granular materials

Jean-Noël Roux

▶ **To cite this version:**

Jean-Noël Roux. The nature of quasistatic deformation in granular materials. R. Garcia-Rojo, H. J. Herrmann, S. McNamara. Powders and Grains 2005, Jul 2005, Stuttgart, Germany. A. A. Balkema, Leiden, pp. 261–265, 2005. <hal-00353569>

HAL Id: hal-00353569
https://hal.archives-ouvertes.fr/hal-00353569

Submitted on 15 Jan 2009

The nature of quasistatic deformation in granular materials

J.-N. Roux

Laboratoire des Matériaux et des Structures du Génie Civil, Institut Navier, Champs-sur-Marne, France

ABSTRACT: Strain in granular materials in quasistatic conditions under varying stress originate in (I) contact deformation and (II) rearrangements of the contact network. Depending on sample history and applied load, either mechanism might dominate. One may thus define rheological regimes I and II accordingly. Their properties are presented and illustrated here with discrete numerical simulation results on sphere packings. Understanding the microscopic physical origin of strain enables one to clarify such issues as the existence of macroscopic elasticity, the approach to stress-strain relations in the large system limit and the sensitivity to noise.

1 INTRODUCTION

Macroscopic strain in solidlike granular materials has two obvious physical origins: first, grains deform near their contacts, where stresses concentrate (so that one models intergranular interaction with a point force); then, grain packs rearrange as contact networks, between two different equilibrium states break, and then repair in a different stable configuration. We refer here respectively to the two different kinds of strains as type I and II. The purpose of the present communication is to delineate the regimes, denoted as I and II accordingly, within which one mechanism or the other dominates, in a simple model material (an assembly of spheres), from discrete numerical simulations. Macroscopic mechanical properties are shown to differ, as well as microscopic variables.

The very small strain elastic response of granular materials belongs to regime I: what is measured then is the macroscopic stiffness of a spring network, each intergranular contact behaving like an elastic element. Such a spring network model is usually adopted on studying vibration modes and elastic moduli (Somfai et al. 2004; Agnolin & Roux 2005). However, elastic-frictional contact networks also comprise plastic elements (sliders), and deform irreversibly under quasistatically applied stress increments. As long as they still support the applied load, strain amplitudes scale as the inverse of the stiffness constants of the springs. Such a scaling will be used here as a signature of regime I, which extends, beyond the quasi-elastic domain, throughout the stress or strain interval corresponding to the elastoplastic response of a given contact network. If grains are modeled as perfectly rigid, strains in regime I reduce to zero.

Regime II will in general correspond to larger strains, for which contact networks keep rearranging. Strain amplitudes are then related to the distances (gaps) between neighbouring grains that do not touch. Contact stiffnesses are then expected to have little influence on macroscopic deformations. Such situations are sometimes studied by simulation methods that deal with rigid grains, such as Contact Dynamics (Radjai & Roux 2004). As the network continuously fails and repairs, larger dynamical effects and larger spatial fluctuations of strain are expected, since failing materials usually exhibit larger heterogeneities.

The simulations reported below explore the conditions of occurrence of regimes I and II, and give a quantitative meaning to the statements made in this introduction. After basic features of numerical computations are introduced in Sec. 2, results on the constitutive law and regimes I and II are given in Sec. 3. Sec. 4 is a brief conclusion.

2 NUMERICAL MODEL

Triaxial compression tests of monosized assemblies of N ($N = 4000$ for most results here). spheres of diameter a were simulated by molecular dynamics (MD, or DEM). In those computer experiments, one starts with an isotropically assembled initial state with pressure P, and then, keeping the axes of coordinates as principal stress directions, increases slowly the largest principal stress, σ_1, while the others are held fixed, equal to P. One denotes as q the stress deviator, $q = \sigma_1 - p$. Like in most numerical studies, we chose here to impose a constant strain rate $\dot{\epsilon}_1$ and to measure σ_1 as a function of ϵ_1, termed "axial strain" and subsequantly denoted as ϵ_a. Soil mechanics conventions are adopted: compressive stresses and shrinking strains are positive. We focus on the quasistatic mechanical behaviour expressed by dependences $q(\epsilon_a)$, $\epsilon_v(\epsilon_a)$ as ϵ_a increases, in dense systems, before the de-

viator peak is reached. ϵ_v is the *volumetric strain* (relative volume decrease). Dimensional analysis leads to the definition of the inertia parameter $I = \dot{\epsilon}_a \sqrt{m/aP}$ as a measure of the departure from equilibrium, the quasistatic limit being $I \to 0$.

Motivated by possible comparisons to laboratory experiments with glass bead packings, simulations are carried out with Hertz-Mindlin contacts, with the elastic properties of glass (Young modulus $E = 70$ GPa, Poisson coefficient $\nu = 0.3$), and a friction coefficient $\mu = 0.3$ – additional details and references are provided in (Agnolin & Roux 2005). Normal viscous forces are also implemented: the damping parameter in any contact is chosen as a fixed fraction ζ of its critical value, defined for the contacting pair with its instantaneous (i.e., dependent on current normal force or h) stiffness constant dF_N/dh. A suitable dimensionless parameter characterizing the importance of elastic deflections h in contacts is $\kappa = (E/P)^{2/3}$ (such that $h/a \sim 1/\kappa$).

3 SIMULATION RESULTS

3.1 *Sample preparation*

In order to obtain dense samples, we first simulated sets of sphere packings prepared by isotropic compression of frictionless granular gases. This results in configurations hereafter denoted as A. A-type configurations have a high coordination number (approaching 6 at low pressure if inactive grains are discarded). They therefore present a large force indeterminacy. We observed (fig. 1) that the raise of deviator q with axial strain in such samples is much faster than in usual experimental results, for which ϵ_a is usually of order 1% to 5% at the deviator peak. Likewise, the onset of dilatancy after the initial contractant strain interval is unusually fast in A samples. This motivated the use of a different preparation procedure, which, although idealized, aims to imitate the effects of vibrations in the assembling of a dense, dry packing of beads. In this method (called C in the sequel), A samples are first dilated (multiplying coordinates by 1.005), then mixed, as by thermal agitation, until each grain has had 50 collisions on average, and finally compressed in the presence of friction to a relativy low pressure, $P = 10kPa$. Higher P values are obtained on further compressing. Fig. 1 compares the behaviour of initial states A and C, in triaxial compression with $P = 100$ kPa ($\kappa \simeq 6000$). Agnolin & Roux (2005) report in these proceedings on the large difference in coordination number between A and C states, where it is much smaller (~ 4.7), while densities are very close. Usual experimental curves, which do not exhibit q maxima or dilatancy before $\epsilon_a \sim 0.01$, are better modelled with C samples. Those experiments are made with, e.g., dry grains assembled in the laboratory. One cannot exclude, however, that samples left to age and anneal for a long time gradually evolve towards better coordinated configurations re-

sembling A ones. One may also assemble the grains in the presence of a lubricant, thereby strongly reducing friction in the initial stage (Agnolin et al. 2005). A-type samples can thus be viewed as ideal models for preparation procedures suppressing friction, while C ones are more appropriate models for laboratory specimens made by pouring, vibrating or tapping. A similar conclusion was reached by Agnolin et al. (2005) in a study of sound propagation velocities.

3.2 *Reproducibility, quasistatic limit*

Stress-strain curves as displayed on fig. 1 should express a macroscopic, quasistatic constitutive law. Sample to sample fluctuations should regress in the large system limit, and the results should be independent on dynamical parameters such as inertia, viscous dissipation, and strain rate, summarized in dimensionless parameters ξ and I. Fig. 2 is indicative of sample to sample fluctuations with 4000 beads. One may notice the very good reproducibility of the curve be-
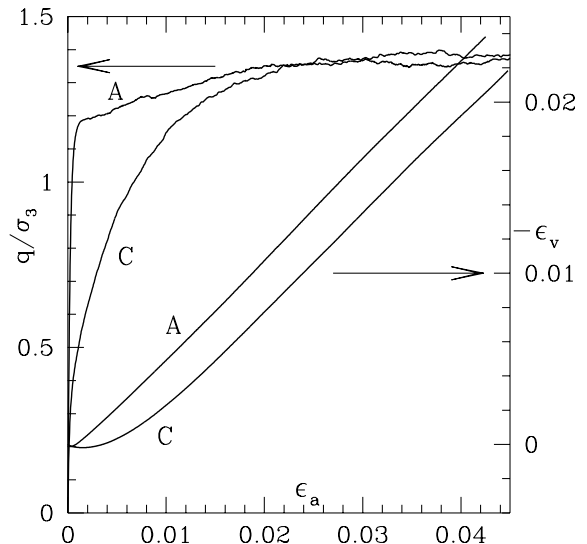

Figure 1. $q(\epsilon_a)$ (left scale) and $\epsilon_v(\epsilon_a)$ (right scale) curves for A and C states under $P = 100$ kPa. Averages over 5 samples of 4000 spherical grains.
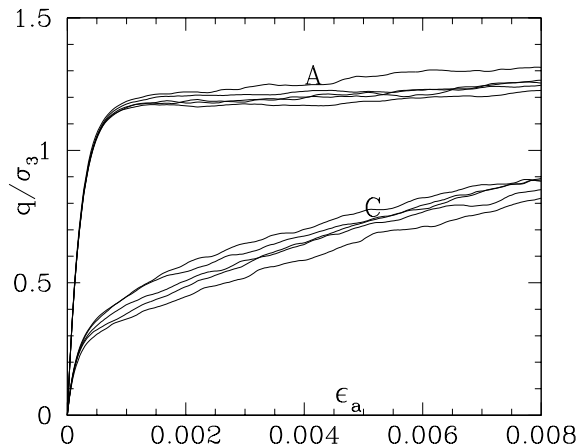

Figure 2. Detail of small strain part of $q(\epsilon_a)$ curves for 5 different samples of each type, A (top curves) and C (bottom ones) with $N = 4000$ beads.

tween A samples in the initial fastly growing part. We checked that differences between samples decreased

for increasing N. As to the influence of dynamical parameters, fig. 3 shows that the quasistatic limit is correctly approached for $I \leq 10^{-3}$, a quite satisfactory result, given that usual laboratory tests with $\dot{\epsilon}_a \sim 10^{-5}$ correspond to $I \leq 10^{-8}$. In previous 2D simulations
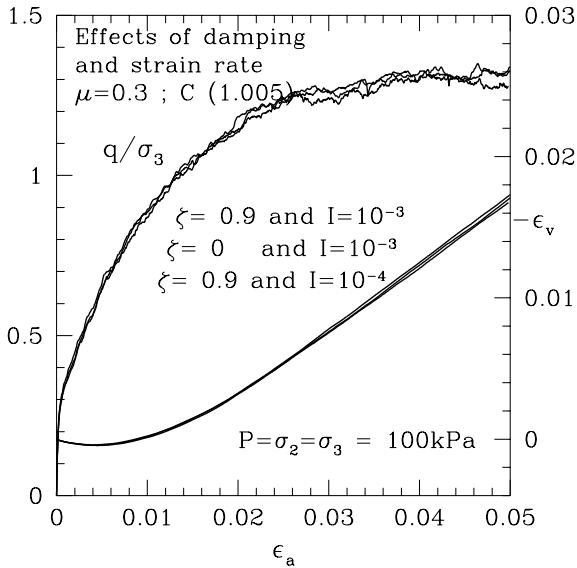

Figure 3. Effect of dynamical parameters: $q(\epsilon_a)$ and $\epsilon_v(\epsilon_a)$ curves for the different values of ζ and I indicated coincide, showing the innocuousness of dynamical parameter choice.

with disks (Roux & Combe 2002), sample to sample fluctuations were shown to regress as $N^{-1/2}$.

3.3 Influence of contact stiffness

The small strain (say $\epsilon_a \leq 5.10^{-4}$) interval for A samples, with its fast q increase, is in fact in regime I. This is readily checked on changing the confining pressure. Fig. 4 shows the curves for triaxial compressions at different P values (separated by a factor $\sqrt{10}$ from 10 kPa to 1 MPa, with a rescaling of the strains by the stiffness parameter κ, in one A sample. Their coincidence for $q/P \leq 0.8P$ evidences a wide deviator range in regime I. For larger strains, curves separate
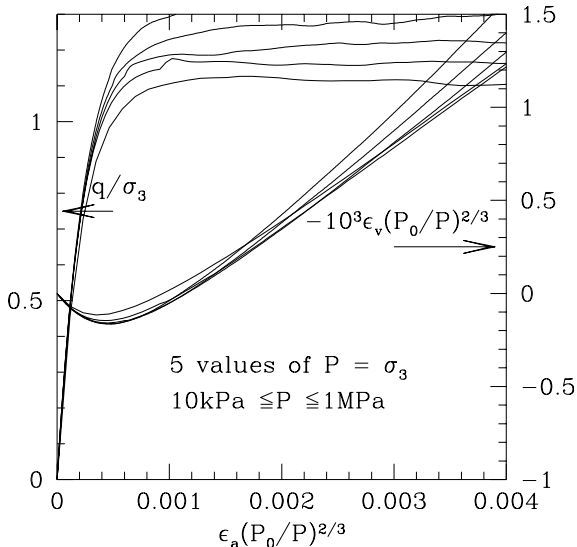

Figure 4. $q(\epsilon_a)/P$ and $\epsilon_v(\epsilon_a)$ curves for one A sample and different P values. Strains on scale $(P/P_0)^{2/3} \propto \kappa^{-1}$, $P_0 = 100$ kPa.

on this scale, and tend to collapse together if q/P, ϵ_v are simply plotted versus ϵ_a. The strain dependence on stress ratio is independent from contact stiffness. This different sensitivity to pressure is characteristic of regime II. Fig 5 shows that it applies to C samples almost throughout the investigated range, down to small deviators (a behaviour closer to usual experimental results than type A configurations). At the origin (close to the initial isotropic state, see inset on fig. 5), the tangent to the curve is given by the elastic (Young) modulus of the granular material, E_m, which scales as κ, but curves quickly depart from this behaviour (below $q = 0.1P$).
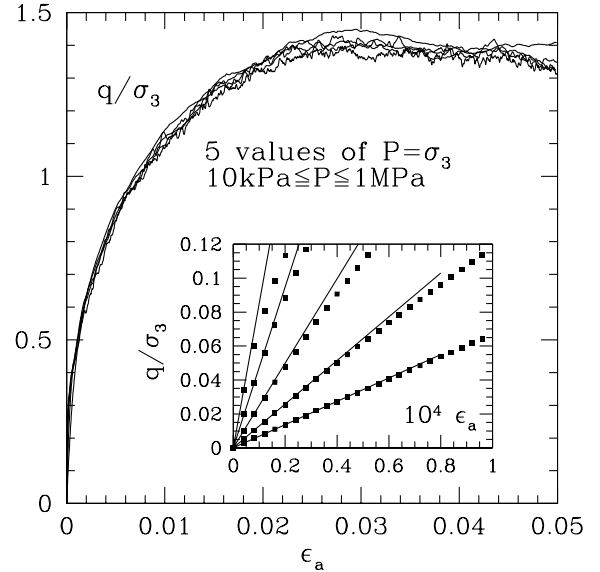

Figure 5. $q(\epsilon_a)/p$ for same p values as on fig. 4, in one C sample. Inset: detail of same curves, blown-up ϵ scale, straight lines corresponding to Young moduli in isotropic state.

3.4 Load reversal

If (fig. 6) one reverses the direction of load increments, the stress-strain curves exhibit notable intervals within which the deviator stress decreases very fast, which results in large irreversible (plastic) strains. It can be checked that the initial slope of those descending curves are equal to the Young modulus E_m of the material, and that subsequent strains scale as $1/E_m$, like the initial q increase in A samples. Therefore, some significant deviator stress intervals (of order $0.2P$ or larger) are found in regime I on reversing deviator stress or axial strain variations.

Fig. 7 shows that the small strain response of A samples, within regime I, close to the initial state, is already irreversible. Type I strains are not elastic.

3.5 Calculations with a fixed contact list

Within regime I, the mechanical properties of the material can be successfully predicted on studying the response of one given set of contacts. Those might slide or open, but the very few new contacts that are created can be neglected. To check this in simulations, one may restrict at each time step the search for interacting grains to the list of initially contacting pairs.
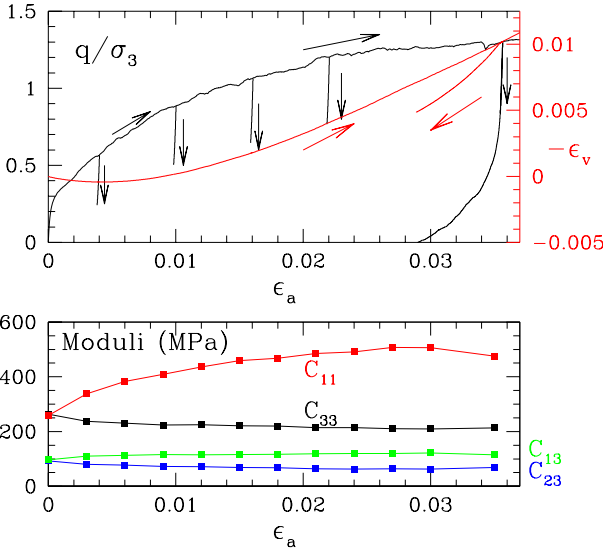
Figure 6. Top plot: effects of load reversals at different points on curves (C sample). Initial slopes of unloading curves correspond to elastic moduli. Bottom: evolution with ϵ_a of some elastic moduli, probing induced anisotropy.
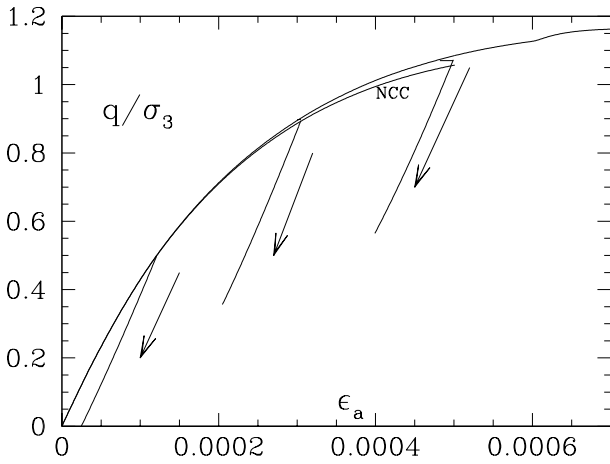
Figure 7. Very small strain part of $q(\epsilon_a)$ curve in one A sample, showing beginning of unloading curves (arrows). Curve marked NCC was obtained on calculating the evolution of the same sample without any contact creation.

Fig. 7 compares such a procedure to the complete calculation. The curve marked "NCC" for *no contact creation* is indistinguishable from the other one for $q \geq 0.8$. In two dimensions, Roux & Combe (2002) could implement a purely static method (elastoplastic computation on a given contact network), apt to calculate the quasistatic evolution of the sample under varying applied stresses throughout the initial regime I stage of 2D assemblies of disks analogous to A samples. The limit between regimes I and II was studied with some accuracy (Combe 2002), and shown to approach a finite value in the rigid limit ($\kappa \to +\infty$), and in the limit of large systems. This value does not appear to depend on details of contact elasticity, such as tangential to normal stiffness ratio (Combe 2002).

3.6 *Microscopic aspects*

The existence of wide stress intervals within regime I is associated with strongly hyperstatic contact networks (large force indeterminacy). Initially, A samples have large coordination numbers, (close to 6)

(Agnolin & Roux 2005), and friction is not mobilized (zero tangential forces). Consequently, the set of contact forces that resolve the load and satisfy Coulomb inequalities is large, and the initial forces are far from its boundaries. At coordination 6 this set spans an affine space of dimension $3N^*$ if N^* is the number of force-carrying particles. In regime II, regarding the Coulomb condition in sliding contacts as a constraint on force values in the count of force indeterminacy, this dimension decreases to a fraction of order 10% of the number of degrees of freedom. Upon reversing the load variation, sliding contacts tend to disappear, leading to a larger force indeterminacy and a notable type I interval. The small variation of coordination number in the pressure range of Fig. 5 (Agnolin et al. 2005) witnesses the smallness of geometrical changes, hence the collapse of curves with type II strains.

Larger strain heterogeneities and sensitivity to perturbations are other characteristic features of regime II (Roux & Combe 2003).

4 CONCLUSION

Numerical studies thus reveal that the two regimes, in which the origins of strain differ, exhibit contrasting properties. On attempting to predict a macroscopic mechanical response from packing geometry and contact laws, the information about which kind of strain should dominate is crucial. Regime I corresponds in usual testing conditions to highly coordinated systems (with many contacts), or to changes in the direction of load increments (hence a loss in friction mobilization). Investigating the nature of strains might open interesting perspectives to study the effects of cyclic loadings or random perturbations.

REFERENCES

Agnolin, I. & Roux, J.-N. 2005. Elasticity of sphere packings: pressure and initial state dependence. These proceedings.

Agnolin, I., Roux, J.-N., Massaad, P., Jia, X., & Mills, P. 2005. Sound wave velocities in dry and lubricated granular packings: numerical simulations and experiments. These proceedings.

Combe, G. 2002. *Mécanique de matériaux granulaires et origines géométriques de la déformation*: Volume SI8 of *Etudes et Recherches des Laboratoires des Ponts et Chaussées*. Paris: Laboratoire Central des Ponts et Chaussées.

Radjai, F. & Roux, S. 2004. Contact dynamics study of 2D granular media : critical states and relevant internal variables. In H. Hinrichsen & D. E. Wolf (eds), *The Physics of Granular Media*: Berlin. Wiley-VCH.

Roux, J.-N. & Combe, G. 2002. Quasistatic rheology and the origins of strain. *C. R. Académie des Sciences (Physique)* 3: 131–140.

Roux, J.-N. & Combe, G. 2003, July. On the meaning and microscopic origins of quasistatic deformation of granular materials. In *Proceedings of the EM03 ASCE conference*: Seattle: paper 759. CD-ROM published by ASCE.

Somfai, E., Roux, J.-N., Snoeijer, J., van Hecke, M., & van Saarloos, W. 2004. Wave propagation in confined granular systems. To appear in Phys. Rev. E, cond-mat 0408128.